Ultrafast gain and refractive index dynamics in GaInNAsSb semiconductor optical amplifiers

T. Piwonski,[1] J. Pulka,[1] G. Madden,[1] G. Huyet,[1] J. Houlihan,[2,a)] J. Pozo,[3] N. Vogiatzis,[3] P. Ivanov,[3] J. M. Rorison,[3] P. J. Barrios,[4] and J. A. Gupta[4]
[1]*Tyndall National Institute, Lee Maltings, Cork, Ireland and Department of Applied Physics, Cork Institute of Technology, Ireland*
[2]*Department of Computing, Maths and Physics, Waterford Institute of Technology, Waterford, Ireland*
[3]*Department of Electrical and Electronic Engineering, University of Bristol, Bristol, BS8 1UB Avon, England*
[4]*Institute for Microstructural Sciences, National Research Council of Canada, Ottawa, Ontario K1A 0R6, Canada*

(Received 25 June 2009; accepted 20 September 2009; published online 22 October 2009)

The gain and refractive index dynamics of dilute nitride antimonide semiconductor optical amplifiers are studied using heterodyne pump probe spectroscopy, both in forward and reverse bias regimes. In the forward biased absorption regime, both gain and refractive index relax on the same timescale indicating that both quantities are linked to the same relaxation process, interband recombination. Above transparency, in the forward biased gain regime, the gain and phase exhibit differing timescales resulting in a dynamical alpha factor that varies strongly with time. Reversed bias measurements suggest a recombination dominated absorption recovery where the recovery timescale increases with increasing reversed bias, possibly due to charge separation effects.
 [doi:10.1063/1.3246781]

I. INTRODUCTION

Dilute nitrides, first proposed by Kondow *et al.*[1] are very attractive materials due to their potential for improved temperature characteristics compared to conventional InP-based based materials used in optical fiber communications systems. The dramatic conduction band bowing due to the addition of nitrogen results in a large conduction band offset relative to GaAs, particularly at 1.3 μm, leading to extremely high characteristic temperatures.[2] A few years later, Yang *et al.*[3] demonstrated that the addition of Sb to dilute nitrides dramatically improves the material and optical quality, reduces the band gap, and modifies the band gap line-up in GaInNAs/GaAs quantum wells (QWs). Significant progress was made in this area,[4–6] leading to room-temperature continuous-wave operation at 1.55 μm and recently single mode GaInNAsSb/GaNAs QW based distributed feedback lasers at the same wavelength were demonstrated.[7] In this paper, we analyze the dynamical properties of the gain and refractive index of GaInNAsSb/GaNAs QW based semiconductor optical amplifiers (SOAs) using pump probe spectroscopy. Such measurements are important to investigate the suitability of this material system to SOA based applications.

II. INVESTIGATED STRUCTURE

The investigated structure is a GaInNAsSb SOA based on a digital alloy GRINSCH laser structure, grown by molecular beam epitaxy.[8] GaInNAsSb lasers fabricated from the same wafer have been extensively studied previously.[9] Briefly, the laser structure was grown on a N^+ GaAs substrate and contains Si (2×10^{18} cm^{-3}) and Be-doped (1×10^{18} cm^{-3}) $Al_{0.33}Ga_{0.67}As$ cladding layers grown at 610 °C. To reduce lateral leakage current and free-carrier absorption, the Si and Be concentrations were reduced to 5×10^{17} and 3×10^{17} cm^{-3} in the 200 and 250 nm cladding regions closest to the waveguide, respectively. Undoped digital-alloy grading was used between the cladding layers and the GaAs waveguide. The active region, grown at 420 °C, nominally consists of two 7 nm $Ga_{0.6}In_{0.4}N_{0.027}As_{0.9605}Sb_{0.0125}$ QWs with 7.5 nm $GaN_{0.045}As_{0.955}$ barriers. A 5 nm intermediate GaAs layer provided a total QW separation of 20 nm. The DQW active region was surrounded by GaAs giving a total thickness of 340 nm to provide a 1λ-waveguide at the 1.55 μm target wavelength. Doped digital-alloy grading was used between the cladding layers and the 100 nm GaAs:Be (1×10^{19} cm^{-3}) and 200 nm GaAs:Si (2×10^{18} cm^{-3}) contact layers. No additional *ex situ* annealing was performed before device fabrication. Initially the semiconductor material was processed into a 0.6 mm long, ridge waveguide laser structure. To reduce the reflectivity of the facets and allow the single pass amplification, Ga-focused ion beam etching was employed (with iodine gas to enhance the etch rate) to create 10° angled facets on the ends of the waveguide. These facets were etched with a high beam current and then polished with a lower beam current. To further reduce reflections, an anti-reflective coating ($R<0.1$ at 1550 nm) was applied to the tilted facets optimized for the effective refractive index of the principal mode (3.2703).

III. SPECTRAL BLUESHIFT

Amplified spontaneous emission (ASE) spectra as a function of current in the pulsed regime were measured at room temperature [Fig. 1(a)]. The peak emission occurred at 1539 nm at a bias of 40 mA in the pulsed regime. A signifi-

a)Electronic mail: jhoulihan@wit.ie.

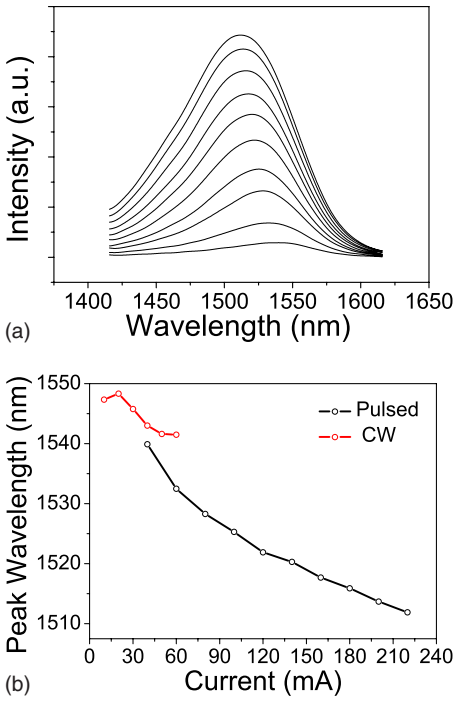

FIG. 1. (Color online) (a) ASE as different current levels (40–220 mA) in the pulsed regime measured at room temperature. (b) Peak emission (ASE) as a function of current in both continuous wave and pulsed regimes.

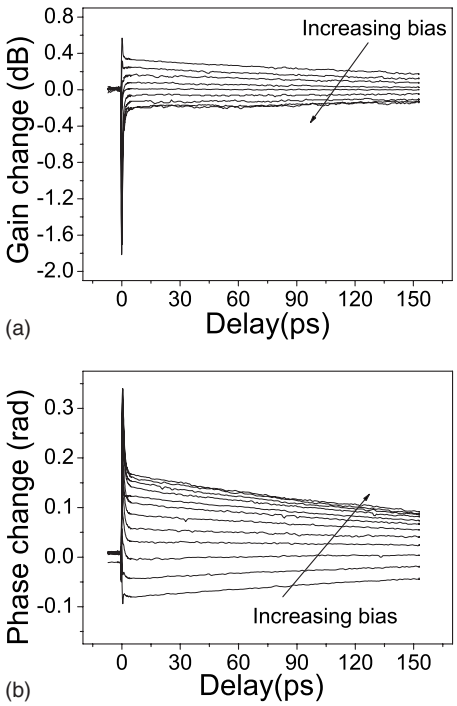

FIG. 2. (a) Gain recovery dynamics as a function of time in the gain and absorption regimes for currents varying from 30 to 90 mA. (b) Corresponding phase recovery dynamics for same conditions. SOA transparency occurs at ≃55 mA.

cant blueshift of the emission peak of approximately 30 nm was observed as the current increased from 40 to 220 mA in the pulsed regime. This blueshift is presented in Fig. 1(b) for both pulsed and cw regimes. However, in cw the onset of lattice heating effects diminishes the overall blueshift. Ishikawa *et al.*[10] reported a similar blueshift for an InGaAsNSb sample. The shift is attributed to the existence of band-tail localized states in the material and their increasing occupation by bound excitons. Such states are a direct consequence of the statistical disorder inherent for quaternary and quinary alloys. As the excitation level increases, these localized states become saturated and a blueshift ensues. They also provided a comparison to a sample without Sb that does not exhibit a blueshift and suggest that the incorporation of Sb induces a deeper localization than would otherwise happen. This may occur as a result of stronger fluctuations of the local potential due to In–Sb bonds, and increased compositional disorder in a quinary alloy compared to a quaternary one.

IV. PUMP-PROBE TECHNIQUE

Single-color time-resolved spectroscopy measurements were performed to investigate the fundamental carrier decay time scales of the device, in both forward bias and reverse bias. Pump-probe differential transmission was measured using a heterodyne detection technique (see Ref. 11 for further details). Briefly, pulses of about 600 fs with a bandwidth of 15 nm at 1539 nm were obtained from a titanium sapphire pumped, optical parametric oscillator and split into three beams: reference, pump, and probe (260 fJ pump pulse energy, 13 fJ probe pulse energy). After propagation through the SOA waveguide with suitable delays, the frequency shifted probe and reference beams were overlapped on a detector, and the amplitude of the difference frequency was detected using a high frequency lock-in amplifier. The resulting signal is proportional to the differential transmission ΔT of a probe pulse at the same wavelength as the pump. The resulting data are represented as the gain change ΔG by the formula $\Delta G = 10 \log(\Delta T / T_0)$, where T_0 is the transmission without pump beam. Measurements were taken at room temperature and performed both as a function of forward bias current and reverse bias voltage. All measurements were obtained in cw mode where the bias induced blueshift is mostly canceled by thermal effects [Fig. 1(b)]. This ensures that the wavelength of the pump and probe beams remained at the peak gain wavelength for the full current range.

V. RESULTS: GAIN DYNAMICS

The dynamics of the carriers in the SOA were investigated in three regimes: gain, absorption, and reverse bias by simultaneous measurement of the gain and phase recovery. Gain dynamics as a function of the delay between the pump and probe pulses, for current values above (gain regime) and below (absorption regime) the transparency current (≃55 mA) are shown in Fig. 2(a). Corresponding phase dynamics are presented in Fig. 2(b).

To perform an analysis of the recovery timescales, the gain dynamics was fitted with a double exponential function. The short time component was found to have a value similar to the pulse width and hence, its analysis is complicated due to the presence of coherent and nonlinear effects, caused by the pump and probe pulses overlapping. Therefore, we focus on the analysis of the timescale and amplitude of the long

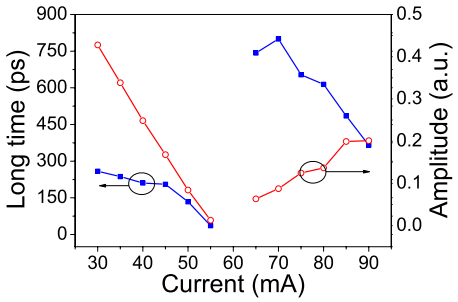

FIG. 3. (Color online) Bias dependence of the long timescale of the gain recovery (blue) and the absolute amplitude (red) of the long timescale component as a function of current for the gain dynamics.

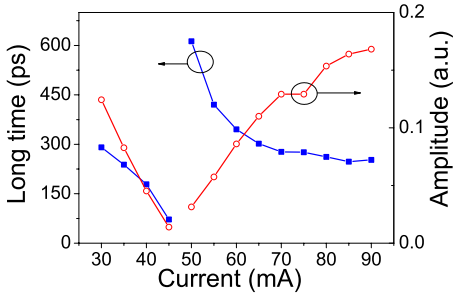

FIG. 4. (Color online) Bias dependence of the long recovery timescale of the phase (blue) and bias dependence of the absolute amplitude of the long time component of the phase (red).

time fitted component of the recovery that may be a limiting factor for switching applications of the device.

Figure 3 shows the fitted long timescale of the gain dynamics (blue) and its absolute amplitude (red) as a function of forward bias current. In general, the long timescale decreases as the injection increases in both the SOA's gain and absorption regimes. However, there is a discontinuity close to the transparency current ($\simeq 55$ mA), where the recovery time shifts abruptly from 40 to 750 ps.

Interestingly, the long timescale of the absorption recovery ($I_{\text{bias}} < 55$ mA) is significantly shorter than that measured in the gain regime. In the absorption regime, the recovery dynamics is governed by the overall interband recombination lifetime (including radiative and nonradiative processes). This recombination lifetime is significantly shorter than those measured in GaAsP based QWs at 1500 nm,[12] most likely as a result of the increased rate of nonradiative recombination due to a higher number of defects in our structure. This conclusion is consistent with measurements of the monomolecular recombination coefficient on the related GaInNAs/GaAs material system.[13] Using a differential carrier lifetime technique based on impedence matching,[14] an order of magnitude increase over conventional GaAs and InP based materials was recorded.

The long timescale in the SOA's gain recovery regime (from 65 to 90 mA) varies from 750 to 370 ps and is similar to those found in other QW structures emitting at 1550 nm, such as those based on GaAsP.[12] In the gain regime, this timescale is commonly related to the replenishment of the carriers into the well from adjacent layers and hence with the relaxation of adjacent layer populations to their steady state levels. In the case of the GaAs layers in the waveguide, these regions have a much lower defect density than the active region layers, and as a result the recombination time in these layers can be much longer than in the active region. Thus, the GaAs region populations can take longer to reach steady state, as does the rate of replenishment to the active region and consequently, the long timescale of the gain recovery of the active region is very similar to those found in conventional, low defect density 1550 mm devices.

VI. RESULTS: PHASE DYNAMICS

The corresponding phase dynamics, as a function of pump-probe delay, is shown in Fig. 2(b) for various currents. As in the gain dynamics case, the phase generally exhibits a double-exponential behavior. The short timescale is similar to that of the gain dynamics. The dependence on bias current of both the long timescale and its absolute amplitude are shown in Fig. 4. A decreasing trend is observed for the recovery time, as seen in the gain dynamics; however, for high currents in the gain regime there is evidence of saturation of its value to 250 ps. No such saturation was present at high currents for the gain dynamics.

To further investigate the phase-amplitude coupling in this structure, the dynamical linewidth-enhancement factor (α-factor) was calculated using the data obtained simultaneously for both gain and phase dynamics according to the formula

$$\alpha = -\frac{4\pi}{\lambda}\frac{\partial n/\partial N}{\partial g/\partial N} = -\frac{4\pi}{\lambda}\frac{\Delta n}{\Delta g},$$

with

$$\Delta n(t) = \frac{\lambda}{2\pi L}\Delta\phi(t), \quad \Delta g(t) = \frac{1}{L}\ln(\Delta G(t))$$

gives

$$\alpha(t) = -\frac{2\Delta\phi(t)}{\ln(\Delta G(t))}, \tag{1}$$

where $\Delta n(t)$ and $\Delta g(t)$ are the pump induced time dependent change in refractive index and change in gain, respectively.

The results of this calculation can be seen in Fig. 5, which shows the time dependence of the linewidth-enhancement factor. The calculation is performed using biexponential fits to the original experimental data to minimize the effects of noise. In the SOA's absorption regime and

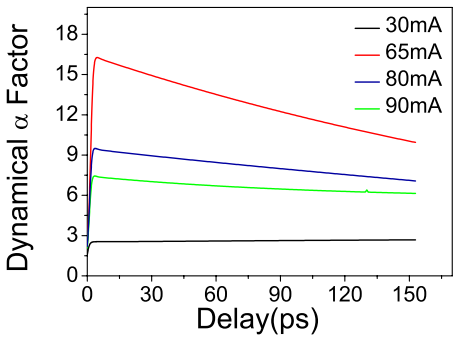

FIG. 5. (Color online) Dynamical alpha factor at different bias levels. Note its decrease above transparency ($\simeq 55$ mA).

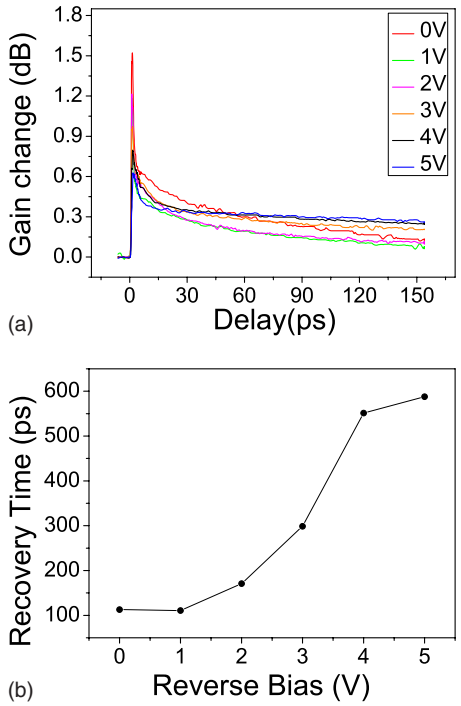

FIG. 6. (Color online) (a) Gain recovery dynamics in reverse bias regime. (b) Long time component recovery times as a function of reverse bias voltage.

apart from the first few picoseconds, its value is constant over time indicating that the phase and gain are linked to the same physical process, i.e., interband recombination. However, above transparency, in the SOA's gain regime, its value changes with time due to clear differences in the long timescales of gain and phase recoveries. This behavior suggests that the gain and refractive index dynamics in the gain regime are linked to different carrier populations and processes. As the injection increases toward 90 mA, these differences appear to reduce as the alpha factor's variation over time reduces. This behavior is consistent with subthreshold Hakki–Paoli measurements of the alpha factor where a reduction with increased bias was recorded.[9] However, the apparent saturation of the phase timescale to 250 ps without saturation of the gain timescale suggests that alpha would exhibit increased variation above 90 mA. Unfortunately, investigation at higher injection levels was not possible for this device.

VII. REVERSED BIAS MEASUREMENTS

The quantum confined Stark effect has previously been analyzed for similar N and Sb based QW materials by Lordi *et al.*,[15] they found large changes in the absorption coefficient with applied bias and concluded that such materials could outperform conventional InP based electroabsorption modulators. To further investigate this point, pump-probe measurements at room temperature were performed in the reverse bias regime (Fig. 6), fitted to a double exponential function and again, we focus on the long time component. Its value increases with increasing reverse bias, as shown on Fig. 7. Similar results were obtained by Malins *et al.*[16] in a dilute nitride structure at 1.3 μm and it was suggested that screening effects may play an important role.[18] This trend is opposite to the one commonly observed in bulk and QW saturable absorbers[17] and more recently for quantum dot absorbers,[18] where in all cases the absorption recovery time decreases as the reversed bias voltage increases. For the QW design employed in these devices, the band offsets between the $Ga_{0.6}In_{0.4}N_{0.027}As_{0.973}$ QW and the $GaN_{0.045}As_{0.955}$ barriers were calculated neglecting the presence of antimony. The resulting values are 81 and 164 meV for the conduction and valence bands, respectively. These are large compared to the thermal energy and suggest that the absorption recovery is dominated by recombination. Consequently, the increase in absorption recovery time with reverse bias may be due to increased charge separation at higher fields and resultant lower recombination rates. More detailed analysis is required to understand the details of such behavior; this will be addressed in a future paper.

VIII. DISCUSSION AND CONCLUSIONS

To summarize, heterodyne pump-probe spectroscopy has been utilized to investigate the gain and refractive index dynamics of GaInNAsSb SOAs. Below transparency in the forward biased absorption regime, both gain and refractive index relax on the same timescale resulting in a constant dynamical alpha factor and indicating that both quantities are linked to the same relaxation process, interband recombination. The timescale of this relaxation process is much shorter than that measured in conventional quantum well devices probably due to the higher defect density in our devices. Above transparency, in the forward biased gain regime, the gain and phase exhibit differing timescales resulting in a dynamical alpha factor that varies strongly with time. The differences reduce as the bias increases, as does the amplitude of the alpha factor. The gain recovery timescale is very similar to that measured in conventional QW devices; this may be linked to replenishment of carriers from similarly low defect density, GaAs barrier layers. It would be interesting to measure the photoluminescence lifetime of these layers to investigate if this was indeed the case. Reverse bias measurements indicate that the recovery timescale increases with increasing reverse bias, a trend similar to recent measurements of a dilute nitride structure. This behavior is linked to lower recombination rates occurring at higher reverse bias fields due to carrier separation effects.

ACKNOWLEDGMENTS

The authors would like to thank Bob Manning for useful discussions, particularly on the reversed bias measurements. This study has been supported by Science Foundation Ireland under the Strategic Research Cluster PIFAS (Grant No. 07/SRC/I1173), the INSPIRE program funded by the Irish Government's Programme for Research in Third Level Institutions, Cycle 4, National Development Plan 2007-2013, and the Institutes of Technology Ireland funding under the Technological Sector Research Strand 1 programme.

[1] M. Kondow, K. Uomi, A. Niwa, T. Kitatani, S. Watahiki, and Y. Yazawa, Jpn. J. Appl. Phys., Part 1 **35**, 1273 (1996).
[2] S. M. Wang, M. Sadeghi, A. Larsson, M. Willander, and J. H. Yang, J.

Appl. Phys. **97**, 073714 (2005).
[3]X. Yang, M. J. Jurkovic, J. B. Heroux, and W. I. Wang, Appl. Phys. Lett. **75**, 178 (1999).
[4]J. A. Gupta, P. J. Barrios, X. Zhang, J. Laponte, G. Pakulski, X. Wu, and A. Delâge, Electron. Lett. **41**, 1060 (2005).
[5]Z. C. Niu, S. Y. Zhang, H. Q. Ni, D. H. Wu, H. Zhao, H. L. Peng, Y. Q. Xu, S. Y. Li, Z. H. He, Z. W. Ren, Q. Han, X. H. Yang, Y. Du, and R. H. Wu, Appl. Phys. Lett. **87**, 231121 (2005).
[6]S. R. Bank, H. P. Bae, H. B. Yuen, M. A. Wistey, L. L. Goddard, and J. S. Harris, Electron. Lett. **42**, 156 (2006).
[7]J. A. Gupta, P. J. Barrios, G. C. Aers, and J. Lapointe, Electron. Lett. **44**, 578 (2008).
[8]J. A. Gupta, G. I. Sproule, X. Wu, and Z. R. Wasilewski, J. Cryst. Growth **291**, 86 (2006).
[9]J. A. Gupta, P. J. Barrios, G. Pakulski, G. C. Aers, J. A. Caballero, D. Poitras, and X. Wu, Proc. SPIE **6485**, S4850 (2007).
[10]F. Ishikawa, Á. Guzmán, O. Brandt, A. Trampert, and K. H. Ploog, J. Appl. Phys. **104**, 113502 (2008).
[11]I. O'Driscoll, T. Piwonski, C.-F. Schleussner, J. Houlihan, G. Huyet, and R. J. Manning, Appl. Phys. Lett. **91**, 071111 (2007).
[12]A. J. Zilkie, J. Meier, M. Mojahedi, P. J. Poole, P. Barrios, D. Poitras, T. J. Rotter, C. Yang, A. Stintz, K. J. Malloy, P. W. E. Smith, and J. S. Aitchison, IEEE J. Quantum Electron. **43**, 982 (2007).
[13]R. Fehse, S. Tomic, A. R. Adams, S. J. Sweeney, E. P. O'Reilly, A. Andreev, and E. Riechert, IEEE J. Sel. Top. Quantum Electron. **8**, 801 (2002).
[14]T. J. Houle, J. C. L. Yong, C. M. Marinelli, S. Yu, J. M. Rorison, I. White, J. K. White, A. J. SpringThorpe, and B. Garrett, IEEE J. Quantum Electron. **41**, 132 (2005).
[15]V. Lordi, H. B. Yuen, S. R. Bank, and J. S. Harris, Appl. Phys. Lett. **85**, 902 (2004).
[16]D. B. Malins, A. Gomez-Iglesias, A. Miller, and M. Guina, Conference on Lasers and Electro-Optics and Quantum Electronics and Laser Science Conference, 4–9 May 2008, San Jose, California, Vols. 1–9, pp. 1690–1691.
[17]J. R. Karin, R. J. Helkey, D. J. Derickson, R. Nagarajan, D. S. Allin, J. E. Bowers, and R. L. Thorntonc, Appl. Phys. Lett. **64**, 676 (1994).
[18]T. Piwonski, J. Pulka, G. Madden, G. Huyet, J. Houlihan, E. A. Viktorov, T. Erneux, and P. Mandel, Appl. Phys. Lett. **94**, 123504 (2009).